

Unitarity in $WW \rightarrow WW$ elastic scattering in topologically massive SU(2) gauge theory

Amitabha Lahiri* and Debmalya Mukhopadhyay†
S. N. Bose National Centre for Basic Sciences,
Block JD, Sector III, Salt Lake,
Calcutta 700 098, INDIA

(Dated: November 26, 2024)

We consider the elastic scattering of longitudinally polarized gauge bosons in an SU(2) generalization of topologically massive gauge theory in four dimensions. We show that the amplitude remains finite at large s , even though the theory does not contain a Higgs particle, in contradiction to common lore.

The Higgs boson [1–3] provides a mechanism of mass generation for gauge bosons. It also plays an important role in maintaining the unitarity of tree-level scattering process among the massive gauge bosons, W . The total amplitude for elastic scattering of longitudinally polarized massive gauge bosons diverges with the increase of energy unless the Higgs particle is included as a mediator [4–7].

Here we consider the topological mass generation mechanism in $3 + 1$ dimensions, in which the mass of the gauge boson is generated without recourse to spontaneous symmetry breaking. The mass is generated via an interaction of the form $B \wedge F$, where B is an antisymmetric 2-tensor potential and F is the field strength of the gauge field [8]. The mass itself is the coupling coefficient of the term and does not appear via any separate mechanism, but is introduced by hand. The resulting theory does not have a Higgs like scalar particle, so it is necessary to check whether unitarity is violated in tree-level processes.

In this model all gauge bosons have the same mass m . The theory can be formulated for any gauge group but for our purposes it is sufficient to consider the group SU(2). Let us label the gauge bosons as W^+ , W^- and W^3 , with

$$W^\pm = \frac{W^1 \mp iW^2}{\sqrt{2}}. \quad (1)$$

Note that W_3 has the same mass as W^\pm

Let us first go over the argument of how unitarity may be violated by a massive triplet of gauge bosons. The tree-level scattering processes involving only the W bosons are shown in Fig. 1.

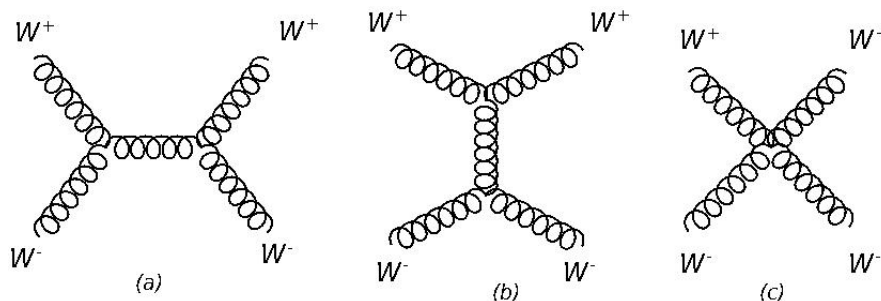


FIG. 1: (a) s-channel, (b) t-channel, (c) direct quartic.

Writing the magnitude of the 3-momentum in the center of momentum frame as P , and the cosine of the angle

between the initial and final W^+ as c , we find that in the high energy limit $P \gg m$, the Feynman amplitudes of these diagrams go as [7]

$$\mathcal{M}_{1s} = -4\frac{g^2 P^4}{m^4}c - 9\frac{g^2 P^2}{m^2}c + O(P^0) \quad (2)$$

$$\mathcal{M}_{1t} = \frac{g^2 P^4}{m^4}(1-c)(3+c) + \frac{g^2 P^2}{2m^2}(9+7c-4c^2) + O(P^0) \quad (3)$$

$$\mathcal{M}_{1q} = -\frac{g^2 P^4}{m^4}(3-6c-c^2) - 2\frac{g^2 P^2}{m^2}(2-3c-c^2) + O(P^0) \quad (4)$$

$$\sum \mathcal{M}_1 = \frac{g^2 P^2}{2m^2}(1+c) + O(P^0). \quad (5)$$

Clearly, if these are the only diagrams for the $W_L^+ W_L^-$ elastic scattering process, the amplitude diverges as $P \rightarrow \infty$ and unitarity is violated. We note that the sum of these amplitudes for the $SU(2) \times U(1)$ gauge theory, when the mediating gauge boson can be either a Z or a photon, may be written in the same form.

Let us see how this divergence is cancelled in the Standard Model. There the masses of the gauge bosons come from the Higgs mechanism, i.e. from a complex scalar doublet. Three of the four modes are converted into the longitudinal modes of the three gauge bosons, and the fourth remains as the Higgs particle H , coupling to W^\pm via a term $mHW_\mu^+ W^{\mu-}$. This leads to two additional diagrams with the Higgs particle as the mediator, shown in Fig. 2, corresponding to amplitudes

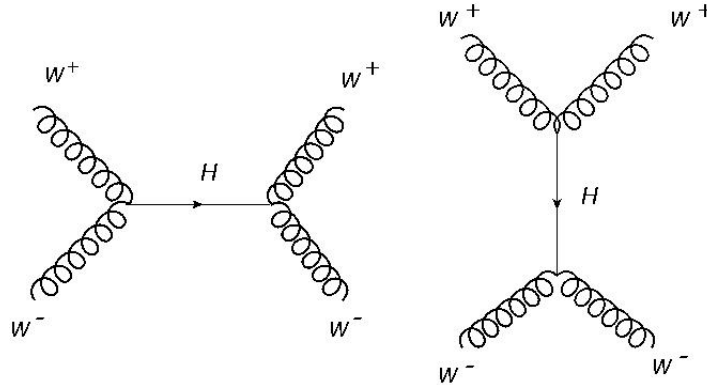


FIG. 2: Higgs-mediated diagrams

$$\mathcal{M}_{2s} = \frac{g^2 P^2}{2m^2}(1-c) + O(P^0) \quad (6)$$

$$\mathcal{M}_{2t} = -\frac{g^2 P^2}{m^2} + O(P^0), \quad (7)$$

so that the total amplitude from the Higgs mediated diagrams cancel the divergence of the previous diagrams, the $W_L^+ W_L^-$ elastic scattering amplitude remains finite, and unitarity is not violated as $P \rightarrow \infty$. A crucial ingredient here was the 3-point coupling between the Higgs and the W particles.

For the topological mass generation mechanism these two diagrams do not appear. However, some new diagrams do appear because of the presence of new fields and interactions. Let us check if the scattering process remains unitary. In this model the mass of the gauge bosons is provided by a coupling of the field with an antisymmetric tensor field $B_{\mu\nu}$. We write the Lagrangian density as

$$\mathcal{L} = -\frac{1}{4}F_a^{\mu\nu}F_{\mu\nu}^a + \frac{1}{12}H_a^{\mu\nu\lambda}H_{\mu\nu\lambda}^a + \frac{m}{4}\epsilon^{\mu\nu\rho\lambda}F_{\mu\nu}^a B_{\rho\lambda}^a \quad (8)$$

Here $F_a^{\mu\nu}$ is the field strength of the gauge bosons

$$F_a^{\mu\nu} = \partial^\mu W_a^\nu - \partial^\nu W_a^\mu - gf_{bca}W_b^\mu W_c^\nu \quad (9)$$

$$= \mathcal{F}_a^{\mu\nu} - gf_{bca}W_b^\mu W_c^\nu \quad (10)$$

with $\mathcal{F}_a^{\mu\nu} = \partial^\mu W_a^\nu - \partial^\nu W_a^\mu$ and the $H_{\mu\nu\lambda}^a$ is the field strength of the second rank anti-symmetric field $B_a^{\mu\nu}$, given by

$$H_a^{\mu\nu\lambda} = \partial^{[\mu} B_a^{\rho\lambda]} - gf_{bca}W_b^{[\mu} W_c^{\rho\lambda]} \quad (11)$$

$$= \mathcal{H}_a^{\mu\nu\lambda} - gf_{bca}W_b^{[\mu} W_c^{\rho\lambda]}, \quad (12)$$

where $\mathcal{H}_a^{\mu\nu\lambda} = \partial^{[\mu} B_a^{\rho\lambda]}$. Here the square brackets represent the cyclic permutation of the indices.

The Lagrangian density of eqn(1) is invariant under $SU(2)$ gauge transformations

$$A_\mu \rightarrow UA^\mu U^{-1} - \frac{i}{g}\partial^\mu UU^{-1} \quad B^{\mu\nu} \rightarrow UB^{\mu\nu}U^{-1} \quad (13)$$

The first term in the Lagrangian density (Eq. 8) provides the 3-point and quartic couplings between the gauge fields. The second term shows WBB and $WWBB$ couplings, where the last term, $B \wedge F$, provides a two point derivative coupling between B and W and a three-point coupling, WWB .

The presence of the $B \wedge F$ term leads to coupled equations of motions in the limit of vanishing gauge coupling $g = 0$

$$\partial_\mu \mathcal{F}_a^{\mu\nu} = -\frac{m}{6}\epsilon^{\nu\rho\sigma\lambda}\mathcal{H}_{\rho\sigma\lambda}^a \quad (14)$$

$$\partial_\mu \mathcal{H}_a^{\mu\rho\sigma} = \frac{m}{2}\epsilon^{\rho\sigma\alpha\beta}\mathcal{F}_{\alpha\beta}^a \quad (15)$$

With the gauge-fixing terms

$$\mathcal{L}_{gf} = -\frac{1}{2\xi}(\partial_\mu A_a^\mu)^2 - \frac{1}{2\zeta}(\partial_\mu B_a^{\mu\nu})^2 \quad (16)$$

and with the exclusion of the $B \wedge F$ coupling, the quadratic terms in eqn(1) yield the propagators of the W_μ^a and $B_a^{\rho\lambda}$

$$i\Delta_{\mu\nu,ab} = -\frac{i}{k^2}\left(g^{\mu\nu} - (1-\xi)\frac{k^\mu k^\nu}{k^2}\right)\delta_{ab} \quad (17)$$

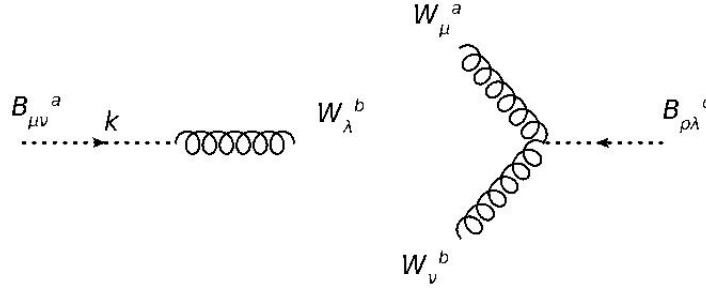
$$i\Delta_{\mu\nu,\rho\lambda;ab} = \frac{i}{k^2}\left(g_{\mu[\rho}g_{\lambda]\nu} - (1-\zeta)\frac{k_\mu k_{[\lambda}g_{\rho]\nu} - k_\nu k_{[\lambda}g_{\rho]\mu}}{k^2}\right)\delta_{ab} \quad (18)$$

The last term in the Lagrangian density gives the vertex rules

$$iV_{\mu\nu,\lambda}^{ab} = -m\epsilon_{\mu\nu\lambda\rho}k^\rho\delta^{ab} \quad (19)$$

$$iV_{\mu,\nu,\lambda\rho}^{abc} = -igmf^{bca}\epsilon_{\mu\nu\lambda\rho}, \quad (20)$$

where the momenta are all directed towards the vertex, and $\delta^{ab} = 2\text{Tr}(t^a t^b)$. In order to use these vertices in a diagram, we need propagators for the fields, which come from kinetic terms, $-\frac{1}{4}\mathcal{F}_{\mu\nu}^a\mathcal{F}^{a\mu\nu}$ for the W bosons,

FIG. 3: Vertices from the $B \wedge F$ term

and $\frac{1}{12}\mathcal{H}_{\mu\nu\lambda}^a\mathcal{H}^{a\mu\nu\lambda}$ for the B field. In the Feynman-'t Hooft gauge, and ignoring the 2-point vertex for the moment, the propagators are

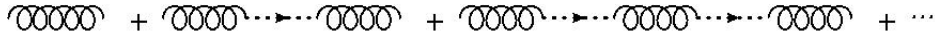
$$i\Delta_{\mu\mu'}^{ab} = \frac{-ig_{\mu\mu'}\delta^{ab}}{k^2 + i\varepsilon} \quad (21)$$

$$i\Delta_{\mu\nu,\mu'\nu'}^{ab} = \frac{ig_{\mu[\mu'}g_{\nu']\nu}\delta^{ab}}{k^2 + i\varepsilon}, \quad (22)$$

where the square brackets indicate antisymmetrization. The effective tree-level propagator for the W boson is the sum over all possible insertions of the B -field [8] as in Fig. 4,

$$\begin{aligned} iD_{\mu\nu} &= i\Delta_{\mu\nu} + i\Delta_{\mu\mu'}\frac{1}{2}iV_{\sigma\rho,\mu'}i\Delta_{\sigma\rho,\sigma'\rho'}\frac{1}{2}iV_{\sigma'\rho',\nu'}i\Delta_{\nu'\nu} + \dots \\ &= \frac{-ig_{\mu\nu}}{k^2 + i\varepsilon} \left(1 + \frac{m^2}{k^2} + \frac{m^4}{k^4} + \dots\right) = \frac{-ig_{\mu\nu}}{k^2 - m^2 + i\varepsilon}, \end{aligned} \quad (23)$$

which is the propagator of a massive vector boson of mass m . The factors of $\frac{1}{2}$ compensate for double-counting due to the antisymmetrization of the indices. We have suppressed the gauge indices here.

FIG. 4: Massive W propagator by summing over B insertions

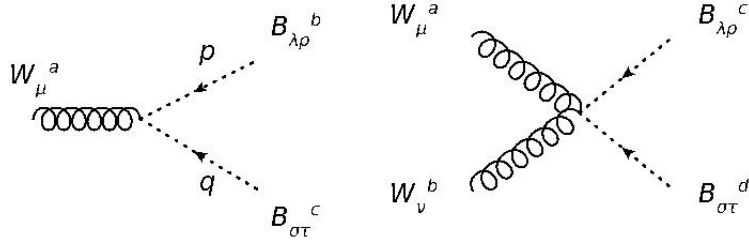
The particle interpretation of quantum fields come from the quadratic part of the Lagrangian. We have made the vector bosons massive by diagonalization of the quadratic terms, with no leftover field degree. The B field has only one degree of freedom per gauge index, which provides the longitudinal mode of the massive gauge boson. Thus the B triplet acts similarly to the Goldstone modes of the complex Higgs field, but the $SU(2)$ symmetry is unbroken. All the three vector bosons have the same mass, and nothing analogous to the Higgs particle appears in the spectrum.

However, the kinetic term for the B field contains new interactions between the B and the W fields. From eq(1) and using the eq(11), we can read off the vertices shown in Fig. 5,

$$iV_{\mu,\lambda\rho,\sigma\tau}^{abc} = gf^{abc} [(p-q)_\mu g_{\lambda[\sigma}g_{\tau]\rho} + p_{[\sigma}g_{\tau][\lambda}g_{\rho]\mu} - q_{[\lambda}g_{\rho][\sigma}g_{\tau]\mu}] \quad (24)$$

$$iV_{\mu,\nu,\lambda\rho,\sigma\tau}^{abcd} = ig^2 [f^{ace}f^{bde} (g_{\mu\nu}g_{\lambda[\sigma}g_{\tau]\rho} + g_{\mu[\sigma}g_{\tau][\lambda}g_{\rho]\nu}) + f^{ade}f^{bce} (g_{\mu\nu}g_{\lambda[\sigma}g_{\tau]\rho} + g_{\mu[\lambda}g_{\rho][\sigma}g_{\tau]\nu})]. \quad (25)$$

Instead of the diagrams of Fig. 2 mediated by the Higgs particle we now find several new diagrams corresponding to $W^+W^- \rightarrow W^+W^-$ scattering at the tree level. We may ignore those which, by power counting, behave as P^0 or less. We have grouped the remaining diagrams into Fig. 6, Fig. 7 and Fig. 8, according to the number

FIG. 5: Vertices from the $H_{\mu\nu\lambda}H^{\mu\nu\lambda}$ term

of internal B propagators. The amplitudes for all of these diagrams go as P^2 . In Fig. 6, diagrams (a) and (b) appear only once, but diagrams (c) and (d) have twins, obtained by exchanging the internal B and W lines. Similarly, the B line can be on any of the external legs in each of diagrams (e) and (f), leading to a multiplicity of 4.

We have calculated the amplitudes corresponding to these diagrams using the vertex rules and propagators given above. For the internal W propagators we have used the resummed propagator of Eq. (23). For internal B propagators we can do a similar resummation, leading again to $k^2 - m^2$ in the denominator. For a B propagator on an external leg, we have used the propagator in Eq. (22). The amplitudes for the diagrams in Fig. 6, including their multiplicities, are

$$\mathcal{M}_{6a} + \mathcal{M}_{6b} = -\frac{3g^2 P^2}{2m^2}(1+c) + O(P^0) \quad (26)$$

$$2(\mathcal{M}_{6c} + \mathcal{M}_{6d}) = \frac{3g^2 P^2}{m^2}(1+c) + O(P^0) \quad (27)$$

$$4(\mathcal{M}_{6e} + \mathcal{M}_{6f}) = -\frac{2g^2 P^2}{m^2}(1+c) + O(P^0). \quad (28)$$

We note that the diagrams in the last row of Fig. 7 have different amplitudes, even though the diagrams themselves appear to be related by exchanges of B and W lines. Including multiplicities, the amplitudes of Fig. 7 are

$$2(\mathcal{M}_{7a} + \mathcal{M}_{7b}) = \frac{2g^2 P^2}{m^2}(1+c) + O(P^0) \quad (29)$$

$$4(\mathcal{M}_{7c} + \mathcal{M}_{7d}) = \frac{4g^2 P^2}{m^2}(1+c) + O(P^0) \quad (30)$$

$$4(\mathcal{M}_{7e} + \mathcal{M}_{7f}) = -\frac{4g^2 P^2}{m^2}(1+c) + O(P^0) \quad (31)$$

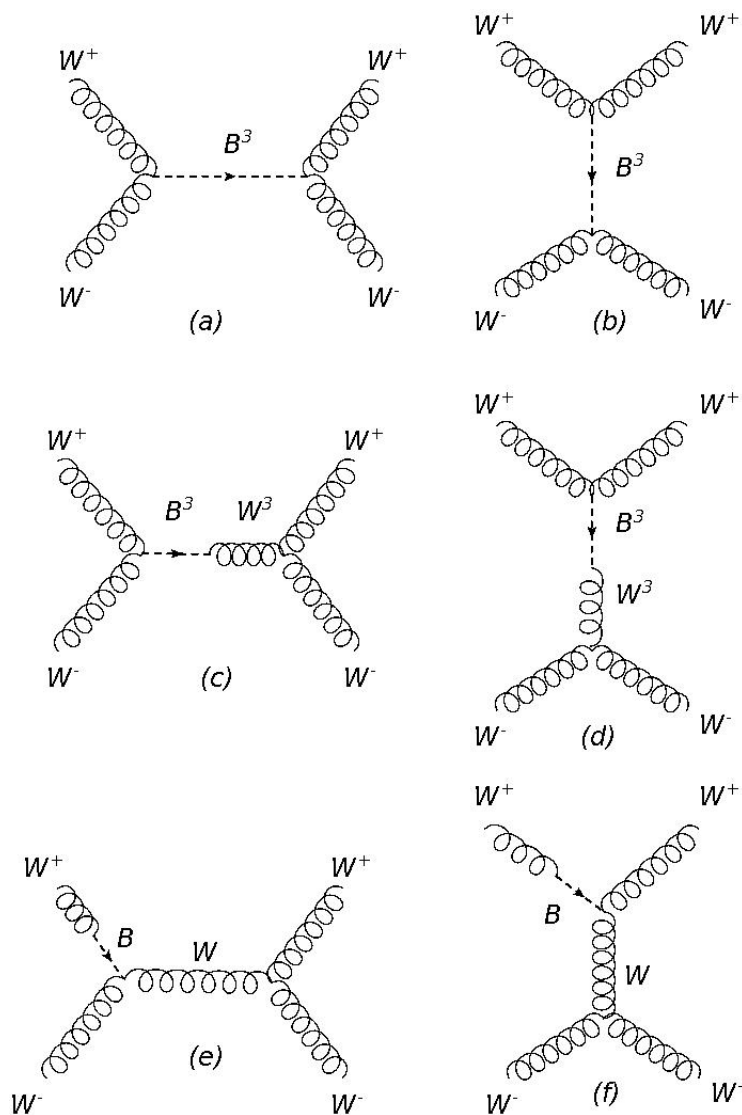
$$2(\mathcal{M}_{7g} + \mathcal{M}_{7h} + \mathcal{M}_{7i}) = \frac{2g^2 P^2}{m^2}(1+3c+2c^2) + O(P^0). \quad (32)$$

The remaining diagrams which go as P^2 are shown in Fig. 8. There are two of each diagram, corresponding to exchanging the B line between the incoming lines and simultaneously between the outgoing lines. The amplitudes for these are

$$2(\mathcal{M}_{8a} + \mathcal{M}_{8b} + \mathcal{M}_{8c} + \mathcal{M}_{8d}) = -\frac{4g^2 P^2}{m^2}(1+2c+c^2) + O(P^0). \quad (33)$$

Adding the amplitudes of the diagrams in Fig. 6, Fig. 7 and Fig. 8, we get

$$\mathcal{M}_6 + \mathcal{M}_7 + \mathcal{M}_8 = -\frac{g^2 P^2}{2m^2}(1+c) + O(P^0), \quad (34)$$

FIG. 6: Scattering diagrams with P^2 behavior: I

which, when added to the amplitudes of the purely W -mediated diagrams of Fig. 1, cancels the P^2 divergence exactly. The $W_L^+ W_L^-$ elastic scattering amplitude remains finite as $P \rightarrow \infty$, and unitarity is not violated. We note that there are other diagrams in this model for the $W_L^+ W_L^-$ elastic scattering process, but all those are of the order P^0 , so do not affect our argument.

The processes, $W_L^+ W_L^+ \rightarrow W_L^+ W_L^+$, $W_L^- W_L^- \rightarrow W_L^- W_L^-$ and $W_L^+ W_L^- \rightarrow W_L^3 W_L^3$ can be shown in a similar manner to be finite at high energy.

This demonstration of unitarity should not come as a great surprise. The action can be written in a form invariant under the Becchi-Rouet-Stora-Tyutin (BRST)-symmetry by using the auxiliary field in a Stueckelberg mechanism [10] for the B -field, which shows that the theory is unitary [9].

It can also be shown [11] that perturbative corrections contribute no new terms to the action, but only to a rescaling, or renormalization, of the couplings and masses.

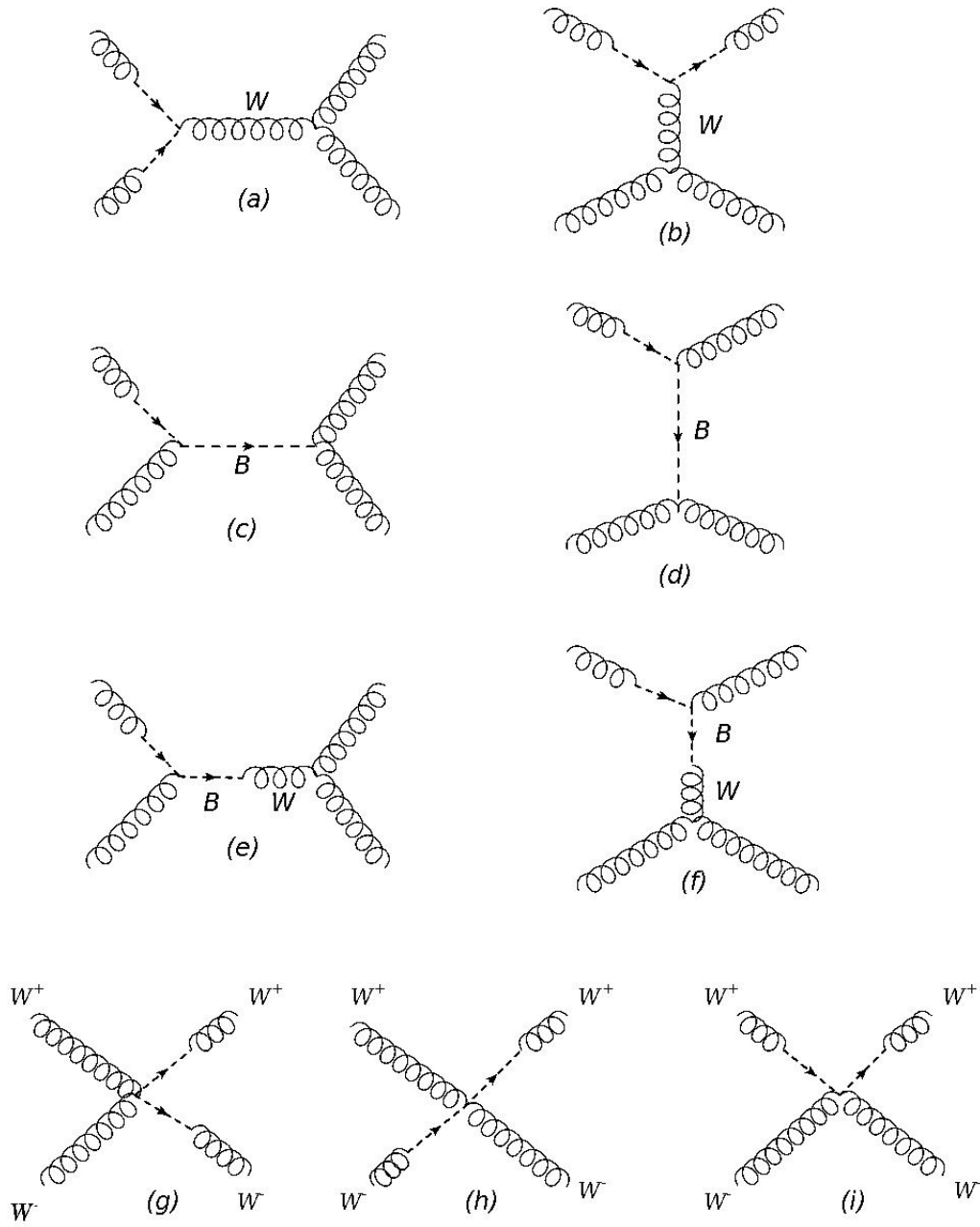


FIG. 7: Scattering diagrams with P^2 behavior: II

We conclude that the topological, or $B \wedge F$, mass generation mechanism for 4-dimension $SU(2)$ gauge theory with the Lagrangian as given in Eq(8) does not violate tree level unitarity of scattering amplitude of longitudinal gauge bosons.

* Electronic address: amitabha@bose.res.in

† Electronic address: debmalya@bose.res.in

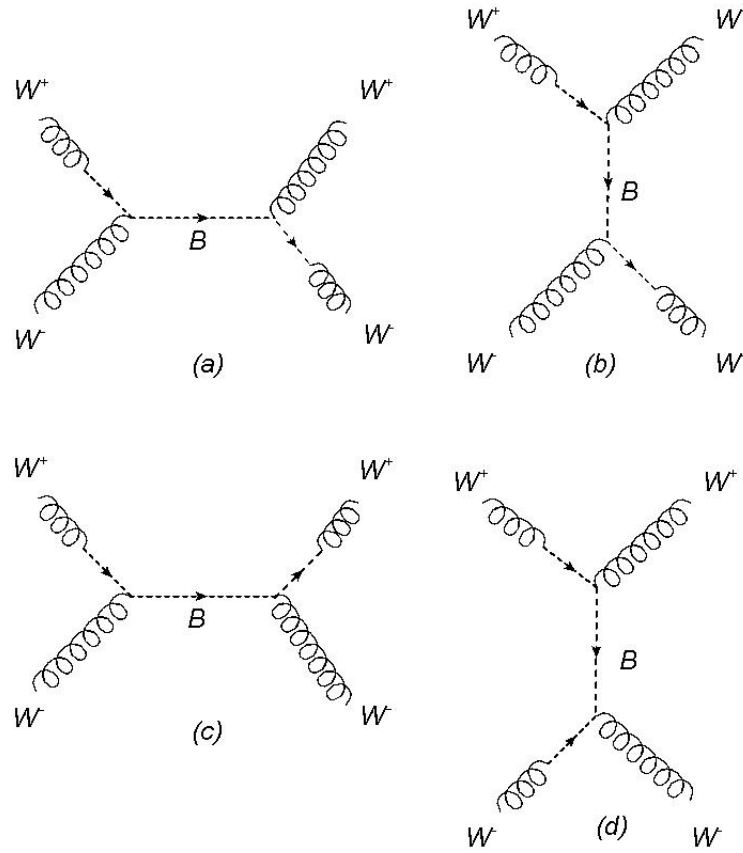


FIG. 8: Scattering diagrams with P^2 behavior: III

- [1] P. W. Higgs, Phys. Rev. Lett. **13**, 508-509 (1964).
- [2] F. Englert, R. Brout, Phys. Rev. Lett. **13**, 321 (1964).
- [3] G. S. Guralnik, C. R. Hagen, T. W. B. Kibble, Phys. Rev. Lett. **13**, 585 (1964).
- [4] C. H. Llewellyn Smith, Phys. Lett. **B46**, 233 (1973).
- [5] J. M. Cornwall, D. N. Levin, G. Tiktopoulos, Phys. Rev. Lett. **30**, 1268 (1973).
- [6] J. M. Cornwall, D. N. Levin, G. Tiktopoulos, Phys. Rev. **D10**, 1145 (1974).
- [7] S. D. Joglekar, Annals Phys. **83**, 427 (1974).
- [8] T. J. Allen, M. J. Bowick, A. Lahiri, Mod. Phys. Lett. **A6**, 559 (1991).
- [9] A. Lahiri, Phys. Rev. **D55**, 5045 (1997).
- [10] H. Ruegg, M. Ruiz-Altaba, Int. J. Mod. Phys. **A19**, 3265 (2004).
- [11] A. Lahiri, Phys. Rev. **D63**, 105002 (2001).